Anal. Calcd for $C_{24}H_{20}SiCr$: C, 74.23; H, 5.15. Found: C, 73.03; H, 5.27.

Preparation of (1-6:1′-6′-η-Tetraphenylsilane)vanadium (7). The synthesis of **7** proceeded in analogy to that of **5**. From 1.2 g (5.8 mmol) of bis(benzene)vanadium (**12**) 0.78 g (2.0 mmol, 35%) of **7** was obtained as glistening black stars. **7** decomposes at 225 °C before melting. MS (m/z (relative intensity)): 387 (M^+, 100), all fragment ions $I < 10\%$. Anal. Calcd for $C_{24}H_{20}SiV$: C, 74.73; H, 5.16. Found: C, 73.77; H, 5.48.

Preparation of Bis((triphenylsilyl)-η⁶-benzene)chromium (6). A 1.3-g (6.3-mmol) amount of bis(benzene)chromium (**9**) was metalated as described above. A 4.45-g (15.1-mmol) portion of chlorotriphenylsilane, dissolved in 100 mL of petroleum ether, was then added to the cooled (0 °C) suspension with vigorous stirring. Filtration followed by partial extraction of the sparingly soluble solid residue with 250 mL of boiling toluene gave 100 mg (1.4 mmol, 2.4% yield) of **6** as a yellow-orange, amorphous powder. MS (m/z (relative intensity)): 724 (M^+, 30), 388 ($M^+ - SiPh_4$, 100), 336 ($SiPh_4^+$, 25), 259 ($SiPh_3^+$, 75), 182 ($SiPh_2^+$, 40), 52 (^{52}Cr, 25). Anal. Calcd for $C_{48}H_{40}Si_2Cr$: C, 79.55; H, 5.52. Found: C, 79.65; H, 5.43.

Preparation of Bis((triphenylsilyl)-η⁶-benzene)vanadium (8). The synthesis of **8** was performed as described for the chromium analogue **6**. From 0.79 g (3.8 mmol) of bis(benzene)vanadium (**12**) 0.24 g (0.33 mmol, 8.7%) of **8** was obtained as maroon microcrystals. MS (m/z (relative intensity)): 723 (M^+, 17), 387 ($M^+ - SiPh_4$, 38), 336 ($SiPh_4^+$, 49), 259 ($SiPh_3^+$, 100), 182 ($SiPh_2^+$, 62). Anal. Calcd for $C_{48}H_{40}Si_2V$: C, 79.64; H, 5.57. Found: C, 79.10; H, 5.88.

Cocondensation of Tetraphenylsilane with Chromium Atoms. A 1-g (3-mmol) amount of tetraphenylsilane (internal vaporization) and 0.52 g (10 mmol) of chromium were cocondensed at −196 °C (10^{-4} mbar) over 1 h. Extraction of the reaction mixture with toluene followed by removal of solvent under reduced pressure yielded an orange solid. According to ^1H NMR spectroscopy this material consists of a mixture of tetraphenylsilane and bis((triphenylsilyl)-η⁶-benzene)chromium (**6**) in an approximate 20:1 ratio. No traces of **5** were found.

Protodesilylation of (1-6:1′-6′-η-tetraphenylsilane)chromium (5). A 50-mg amount of **5** (0.13 mmol) was dissolved in 50 mL of warm THF, giving a clear red-orange solution. To this was added 2.5 mL of N_2-saturated water. Within minutes, the solution turned yellow. Filtration through activated alumina and removal of solvent under reduced pressure, followed by recrystallization from ligroin, yielded 20 mg of a light tan powder, which was subjected to ^1H and ^{13}C NMR and mass spectral analysis. MS (m/z (relative intensity)): 794 (**10**$^+$, 17). ^1H NMR (C_6D_6): δ 7.85 (doublet of doublets, relative intensity 1), 7.71 (doublet of doublets, 4.2), 7.20 (m, 12), 4.23 (s, 6.5). ^{13}C NMR (C_6D_6): δ 136.9 (C_{meta}), 134.8 (C_{para}), 130.9 (C_{ipso}), 129.9 (C_{meta}), 74.8 (**9**). From this analysis, it is apparent that the product is a mixture of primarily bis(benzene)chromium (**9**), poly(diphenylsiloxane), and traces of **10**.

Acknowledgment. We thank the Deutsche Forschungsgemeinschaft (DFG) and the donors of the Fonds der Chemischen Industrie for the support of this work. J.H. is indebted to Deutscher Akademischer Austauschdienst (DAAD) for the award of a scholarship.

Registry No. **5**, 125594-40-3; **6**, 125594-41-4; **7**, 125594-42-5; **8**, 125594-43-6; **9**, 1271-54-1; **11**, 1048-08-4; **12**, 12129-72-5; Cr, 7440-47-3; Ph_2SiCl_2, 80-10-4; Ph_3SiCl, 76-86-8; bis(1-lithiobenzene)chromium, 125594-39-0; poly(diphenylsiloxane), 775-12-2.

Supplementary Material Available: A table of anisotropic temperature factors and atomic coordinates of the H atoms and a complete list of bond lengths and angles (3 pages); a table of the structure factors (9 pages). Ordering information is given on any current masthead page.

Theoretical Study of $Cp_2Ti(H)(SiH_3)$ and Cp_2TiSiH_2 and Their Possible Role in the Polymerization of Primary Organosilanes

John F. Harrod,† Tom Ziegler,*,‡ and Vincenzo Tschinke‡

Departments of Chemistry, McGill University, Montreal, Quebec H3A 2K6, Canada, and University of Calgary, Calgary, Alberta T2N 1N4, Canada

Received May 11, 1989

The two reactions $Cp_2Ti(H)(SiH_3) \rightarrow Cp_2Ti{=}SiH_2 + H_2$ and $Cp_2Ti{=}SiH_2 + SiH_4 \rightarrow Cp_2Ti(H)SiH_2SiH_3$ have been modeled with use of density functional theory and the HFS–LCAO program system by Baerends et al. Both kinetic and thermodynamic features of these reactions were studied, and the results of the computations indicate that the first reaction can proceed with a moderate activation barrier of ca. 60 kJ mol^{-1} and an enthalpy of ca. 40 kJ mol^{-1}. The second reaction is found to be exothermic (ca. −48 kJ mol^{-1}) with an activation barrier of ca. 12 kJ mol^{-1}. The previously proposed mechanism for the titanocene-catalyzed dehydrocoupling of organosilanes is evaluated in terms of these calculations, and it is concluded that the α-hydride elimination–silane addition route is viable. The structural and thermodynamic parameters for each of the important reaction intermediates are also calculated.

I. Introduction

It has recently been shown that the polymerization of primary organosilanes[1] can be catalyzed by dehydrocoupling under the influence of titanocene-based catalysts, according to eq 1.

$$n\mathrm{RSiH_3} \rightarrow \mathrm{RH_2Si[SiRH]_{n-2}SiH_2R} + (n-1)\mathrm{H_2} \quad (1)$$

This reaction is close to thermodynamically neutral. The enthalpy for the elementary dimerization reaction

$$\mathrm{RSiH_3} + \mathrm{R'SiH_3} \rightarrow \mathrm{RH_2SiSiH_2R'} \quad (2)$$

can be estimated with use of literature bond energy values[2] as

$$\Delta H_2 = 2[D(\mathrm{Si{-}H})] - D(\mathrm{H{-}H}) - D(\mathrm{Si{-}Si})$$
$$= (786 - 432 - 340)\ \mathrm{kJ\ mol^{-1}} = 14\ \mathrm{kJ\ mol^{-1}}$$

† McGill University.
‡ University of Calgary.

(1) (a) Aitken, C.; Harrod, J. F.; Samuel, E. *J. Organomet. Chem.* **1985**, 279, C11. (b) Aitken, C.; Harrod, J. F.; Samuel, E. *J. Am. Chem. Soc.* **1986**, 108, 4059. (c) Harrod, J. F.; Yun, S. S. *Organometallics* **1987**, 6, 1381. (d) Aitken, C.; Harrod, J. F.; Samuel, E. *Can. J. Chem.* **1986**, *64*, 1677. (e) Aitken, C.; Harrod, J. F.; Gill, U. S. *Can. J. Chem.* **1987**, *65*, 1804. (f) Harrod, J. F. *ACS Symp. Ser.* **1988**, *No. 360*, 89. (g) Harrod, J. F. In *Transformation of Organometallics into Common and Exotic Materials: Design and Activation*; Laine, R. M., Ed.; NATO ASI Series, Series E, No. 141; Kluwer: Boston, MA, 1988; p 103.

0276-7333/90/2309-0897$02.50/0

This slight endothermicity is probably overcome by the easy loss of hydrogen from the system.

It was proposed[1f] that the key intermediate in the chain-propagation step is $Cp_2Ti(H)(SiH_2R)$ and that this intermediate may undergo an α-hydride elimination to give a molecule of hydrogen and a silylene complex of titanocene:

$$Cp_2Ti(H)(SiH_2R) \rightarrow Cp_2Ti{=}SiHR + H_2 \quad (3)$$

Chain extension was the proposed to occur by addition of a molecule of $RSiH_3$ across the silylene–metal bond (eq 4).

$$Cp_2Ti{=}SiHR + RSiH_3 \rightarrow Cp_2Ti(H)(SiHRSiH_2R) \quad (4)$$

Although silylene complexes of other metals have been reported,[3,4] such complexes of titanium are hitherto unknown.

The theoretical study reported in the present paper is based on density functional theory[5] and the HFS–LCAO program system of Baerends[6] et al. The study had two objectives, the first of which was to analyze the thermodynamics of the two postulated steps (3) and (4) by using the model reactions

$$Cp_2Ti(H)(SiH_3) \rightarrow Cp_2TiSiH_2 + H_2 \quad (5)$$

$$Cp_2TiSiH_2 + SiH_4 \rightarrow Cp_2Ti(H)(SiH_2SiH_3) \quad (6)$$

The second objective was to study the molecular and electronic structures of the reactive silylene ($Cp_2Ti{=}SiHR$) and the hydridosilyltitanocene ($Cp_2Ti(H)(SiH_3)$) complexes, neither of which has been characterized experimentally.

We shall finally carry out exploratory calculations on the reaction profiles for the two model processes in order to get an estimate (upper bound[7]) of the activation barriers.

II. Computational Details

The calculations presented here were carried out with the LCAO–HFS program system developed by Baerends[6] et al. and recently vectorized by Ravenek.[6d] Extensive use has been made of the numerical integration scheme developed by Becke.[8] Bond energies were evaluated by the generalized transition state method,[9] and geometry optimizations were carried out according to the algorithm developed by Versluis[10] and Ziegler. Total energies, E, were evaluated according to

$$E = E_{HFS} + E_c + E_X^{NL} \quad (7)$$

Here E_{HFS} is the total statistical energy expression for the Hartree–Fock–Slater (HFS) or Xα method[11] and E_c and E_X^{NL} are additional correction terms. The first correction term, E_c, has been proposed by Stoll[12] et al. It represents correlation between electrons of different spins, which is lacking in the original HFS method. The second correction term, E_X^{NL}, has been proposed by Becke[13] and represents a nonlocal correction to the local HFS exchange energy. The correction term E_c was based on Vosko's parametrization[14] from electron gas data. The molecular orbitals were expanded as a linear combination of Slater type orbitals (STO).[6] An uncontracted triple-ζ STO basis set[15] was employed for the transition metals. The basis set on the ligands was of double-ζ quality. For Si the basis was augmented by a single STO d orbital ($\zeta_{3d}^{Si} = 1.3$). For all H atoms not on the Cp rings a 2p polarization STO function of $\zeta_{2p}^{H} = 1.0$ was used. A set of auxiliary[16] s, p, d, f, and g STO functions, centered on all nuclei, was used in order to fit the moleculr density and present Coulomb and exchange potentials accurately in each SCF cycle. The orbitals in the upper 3s, 3p, 3d, 4s, and 4p shells on Ti and the upper ns and np shells on the main-group atoms were considered as valence, whereas orbitals in shells of lower energies were considered as core and frozen according to the procedure by Baerends[6] et al. Standard geometries were adopted for C_5H_5 (Cp). The exchange factor[6] α_{ex} in the expression for E_{HFS} was given a value of $^2/_3$ in accordance with Becke's theory.[5] Calculations on metal carbonyls,[17] binuclear metal complexes,[18] and alkyl and hydride complexes,[19] as well as complexes containing M–L bonds for a number of different ligands,[20] have shown that the calculations based on the energy expression given in eq 7 afford metal–ligand and metal–metal bond energies of nearly chemical accuracy (±5 kcal mol^{-1}). Approximate density function methods have also been tested in connection with vibrational frequencies,[21] conformational energies,[22] and triplet–singlet separations.[23] More than 50 molecular structures optimized by approximate density functional theory have been compared with experimental structures.[10] The agreement between experimental and approximate density functional structures is in most cases excellent.

III. Electronic Structure of $(C_5H_5)_2Ti$ and $(C_5H_5)_2Ti(H)(SiH_3)$

The frontier orbitals of the Cp_2Ti d^2 system (**1**) has been studied by Lauher[24] and Hoffmann. The coordinatively unsaturated d^2 fragment of C_{2v} point-group symmetry has three nearly degenerate[25] d-based frontier orbitals, $1a_1$ (**2a**), $1b_1$ (**2b**), and $2a_1$ (**2c**).

We have found the Cp_2Ti has a $^3B_1$ ground state with the electronic configuration $(1a_1)^1(1b_1)^1$. The optimized

(2) Greenwood, N. N.; Earnshaw, A. In *Chemistry of the Elements*; Pergamon Press: Oxford, 1984.
(3) Straus, D. A.; Tilley, T. D.; Rheingold, A. L.; Geib, S. J. *J. Am. Chem. Soc.* **1987**, *109*, 5872.
(4) Zybill, C.; Muller, G. *Organometallics* **1988**, *7*, 1368.
(5) Becke, A. D. *J. Chem. Phys.* **1986**, *84*, 4524.
(6) (a) Baerends, E. J.; Ellis, D. E.; Ros, P. *Chem. Phys.* **1973**, *2*, 71. (b) Baerends, E. J.; Ros, P. *Int. J. Quantum Chem., Quantum Chem. Symp.* **1978**, S12, 169. (c) Baerends, E. J.; Snijders, J. G.; de Lange, C. A.; Jonkers, G. In *Local Density Approximations in Quantum Chemisty and Solid State Physics*; Dahl, J. P., Avery, J., Eds.; Plenum: New York, 1984. (d) Ravenek, W. In *Algorithms and Applications on Vector and Parallel Computers*; te Riele, H. J. J., Dekker, Th. J., van de Vorst, H. A., Eds.; Elsevier: Amsterdam, 1987.
(7) The estimated barriers are upper bounds, as they are determined from a nonoptimized path connecting two optimized local minima on the energy surface.
(8) Becke, A. D. *J. Chem. Phys.* **1988**, *88*, 2547.
(9) Ziegler, T.; Rauk, A. *Theor. Chim. Acta* **1977**, *46*, 1. The generalized transition state method is not only applicable to the HFS scheme. It can be extended to any energy density functional such as the one by Becke in ref 13.
(10) Versluis, L.; Ziegler, T. *J. Chem. Phys.* **1988**, *88*, 322.
(11) Slater, J. C. *Adv. Quantum Chem.* **1972**, *6*, 1.
(12) Stoll, H.; Golka, E.; Preuss, H. *Theor. Chim. Acta* **1980**, *55*, 29.
(13) Becke, A. D. *J. Chem. Phys.* **1986**, *84*, 4524.
(14) Vosko, S. H.; Wilk, L.; Nusair, M. *Can. J. Phys.* **1980**, *58*, 1200.
(15) (a) Snijders, G. J.; Baerends, E. J.; Vernooijs, P. *At. Nucl. Data Tables* **1982**, *26*, 483. (b) Vernooijs, P.; Snijders, G. J.; Baerends, E. J. Slater type basis functions for the whole periodic system. Internal Report; Free University: Amsterdam, The Netherlands, 1981.
(16) Krijn, J.; Baerends, E. J. Fit functions in the HFS-method. Internal Report (in Dutch); Free University: Amsterdam, The Netherlands, 1984.
(17) Ziegler, T.; Tschinke, V.; Ursenbach, C. *J. Am. Chem. Soc.* **1987**, *109*, 4825.
(18) Ziegler, T.; Tschinke, V.; Becke, A. *Polyhedron* **1987**, *6*, 685.
(19) (a) Ziegler, T.; Tschinke, V.; Becke, A. *J. Am. Chem. Soc.* **1987**, *109*, 1351. (b) Ziegler, T.; Cheng, W.; Baerends, E. J.; Ravenek, W. *Inorg. Chem.* **1988**, *27*, 3458. (c) Ziegler, T.; Tschinke, V.; Baerends, E. J.; Snijdes, J. G.; Ravenek, W. *J. Phys. Chem.* **1989**, *93*, 3050.
(20) Ziegler, T.; Tschenke, V.; Versluis, L.; Baerends, E. J.; Ravenek, W. *Polyhedron* **1988**, *7*, 1625.
(21) Fan, L.; Versluis, L.; Ziegler, T.; Baerends, E. J.; Ravenek, W. *Int. J. Quantum Chem., Quantum Chem. Symp.* **1988**, *S22*, 173.
(22) Versluis, L.; Ziegler, T.; Baerends, E. J.; Ravenek, W. *J. Am. Chem. Soc.* **1989**, *111*, 2018.
(23) Ziegler, T.; Rauk, A.; Baerends, E. J. *Theor. Chim. Acta* **1977**, *43*, 261.
(24) Lauher, J. W.; Hoffmann, R. *J. Am. Chem. Soc.* **1976**, *98*, 1729.
(25) The orbital energies for $1a_1$, $1b_1$, and $2a_1$ were calculated to be −2.29, −2.27, and −2.21 eV, respectively.

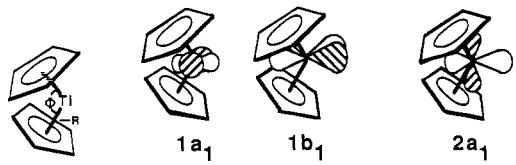

1 2a 2b 2c

structure for the triplet ground state had a Φ value for 1 of 180° and an R value for 1 of 2.04 Å. The first excited state was calculated to be the $^1A_1$ singlet with the $(1a_1)^2$ configuration. The optimized structure of $^1A_1$ is very similar to that of the triplet ground state with Φ = 180° and R = 2.05 Å. The $^1A_1$ state is 70 kJ mol^{-1} higher in energy than $^3B_1$.

The bonding in the d^0 hydrido silyl complex CpTi(H)(SiH_3) (**3a**), with C_s point-group symmetry, can be understood readily in terms of the Cp_2Ti fragment orbitals **2a–2c**, as well as the valence orbitals of H ($1s_H$) and SiH_3 ($2\sigma_{SiH_3}$, $\Pi_{SiH_3}{}^x$, and $\Pi_{SiH_3}{}^y$). The orbitals of importance for

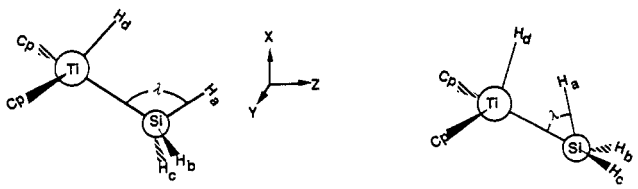

3a 3b

the bonding between Cp_2Ti and the two ligands H and SiH_3 are **4a–4c**, where **4a** and **4b** account for the Ti–H and Ti–Si σ-bonds in **3a** whereas **4c** represents a stabilizing donation from the occupied $\Pi_{SiH_3}{}^x$ orbital to the Ti-based $1a_1$ orbital (**2a**). The energies of **4a–4c** are given on the left side of Figure 1.

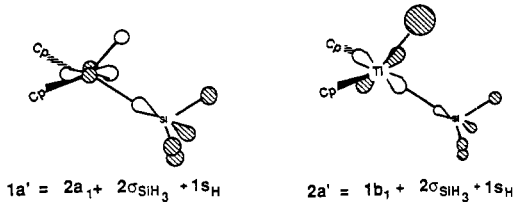

4a 4b

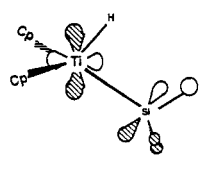

4c

The optimized structure of **3a** is displayed in Figure 2A. The unique hydrogen on the SiH_3 group does not exhibit any agostic behavior, and the three Si–H bond distances are quite similar.

The total enthalpy for the reaction

$$TiCp_2 + H + SiH_3 \rightarrow Cp_2Ti(H)(SiH_3) \qquad (8)$$

was calculated to be −370.5 kJ mol^{-1}. The individual Ti–H and Ti–SiH_3 bond energies were calculated to be D_e(Ti–H) = 245.6 kJ mol^{-1} and D_e(Ti–SiH_3) = 124.9 kJ mol^{-1} in the case where H is disrupted from $Cp_2Ti(H)(SiH_3)$ before SiH_3. The reverse process, where SiH_3 is disrupted before H, gave D_e(Ti–H) = 257.1 kJ mol^{-1} and D_e(Ti–SiH_3) = 113.4 kJ mol^{-1}. The Ti–SiH_3 bond is in both cases seen to be considerably weaker than the Ti–H bond. We note finally that the addition of SiH_4 to $TiCp_2$ is calculated to be an exothermic process with a reaction enthalpy of −41.4 kJ mol^{-1}.

IV. Elimination of H_2 from $Cp_2Ti(H)(SiH_3)$ and the Electronic and Molecular Structure of the Silylene Complex $Cp_2Ti(SiH_2)$

As already mentioned, it has been suggested[1] that the H_2 elimination from CpTi(H)(SiH_3) in eq 5 is a key step in the titanocene-catalyzed silane polymerization. The process in eq 5 can be viewed as a migration of the H_a atom in **3a** toward the H_d ligand with the subsequent formation of the silylene dihydrogen adduct **3d**, from which H_2 is eliminated with the formation of the reactive silylene species **3a**.

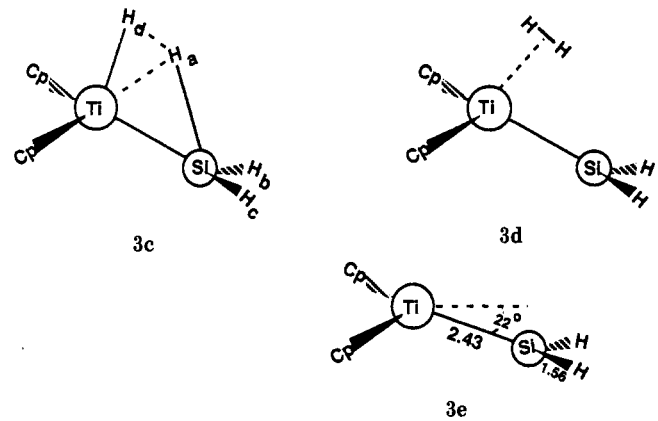

3c 3d

3e

To test the viability of this hypothesis, we have carried out calculations on the molecular and electronic structure of the silylene complex **3e** as well as the reaction enthalpy for the process in eq 5. We have further attempted to trace the reaction profile for the key step in eq 5. It is not computationally feasible at the present time to explore the entire reaction surface for the process in eq 5. Our suggested reaction profile is, as a consequence, approximate, and the calculated activation barriers will constitute upper bounds to the actual barriers.

Calculation on Cp_2TiSiH_2 revealed (**3e**) a relatively short Ti–SiH_2 bond with R(Ti–SiH_2) = 2.43 Å, compared to R(Ti–SiH_3) = 2.68 Å in **3a**. The short Ti–Si distance is indicative of a double bond established by the two interactions **5a** and **5b**, where **5a** represents the σ-bonding Ti–SiH_2 interaction between $1b_1$ (**2b**) of Cp_2Ti and σ_{SiH_2}, whereas **5b** accounts for the Ti–silylene π-interaction between $1a_1$ (**2a**) and the nonbonding 3p orbital on Si.

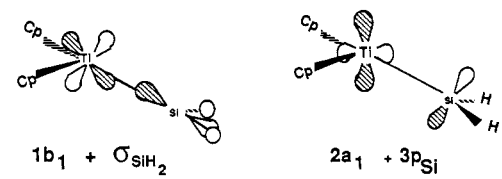

5a 5b

The structure **3a** represents an energy minimum on the energy potential with a positive Hessian matrix. The normal mode of lowest frequency, which could possibly lead toward the product **3d**, is represented by the rocking mode of the SiH_3 group in which the angle λ of **3a** is changed. Thus, this mode was chosen as the reaction coordinate for the initial stages of the process in eq 5. We have as a consequence carried out a rotation of the SiH_3 ligand in which the angle λ of **3a** is changed from λ = 113° to λ = 50° while the H_a atom remains in the symmetry

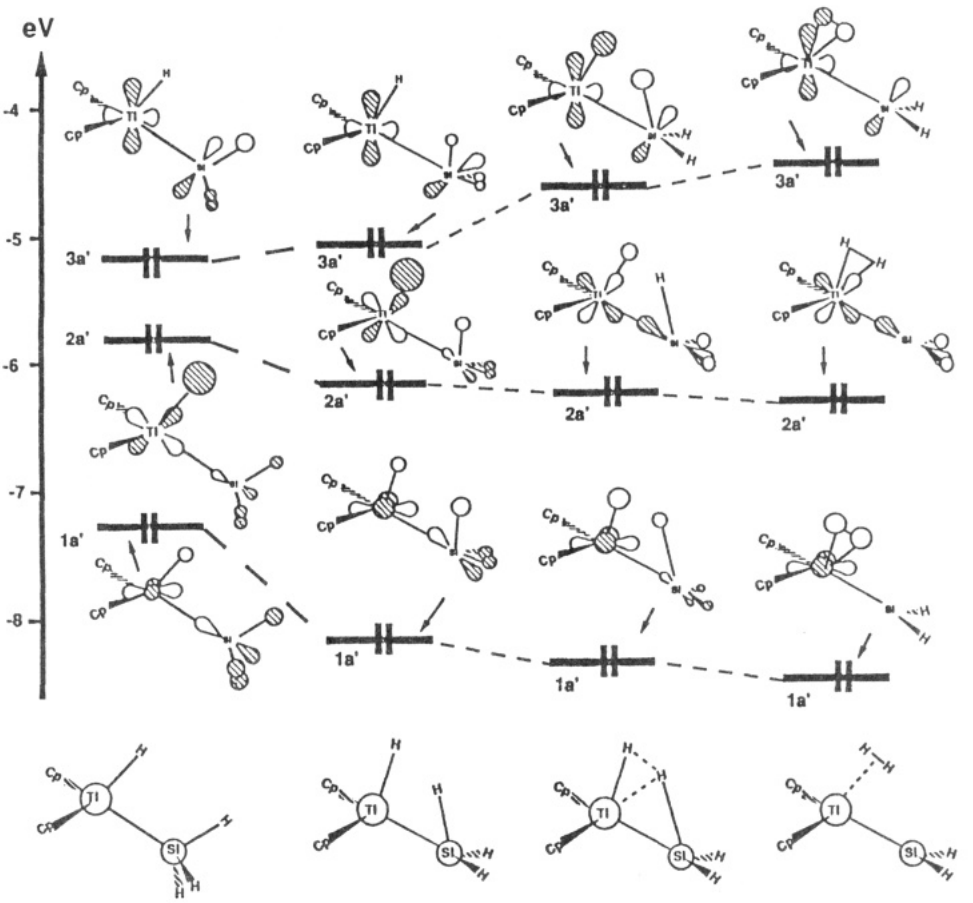

Figure 1. Correlation diagram for the occupied 1a′, 2a′, and 3a′ orbitals in the process **3a** → **3d**. Orbitals of the hydrido silyl complex **3a** are shown to the left and the orbitals of the silylene dihydrogen adduct **3d** to the right.

plane of the $Cp_2Ti(H)(SiH_3)$ species. This rotation leads to the new intermediate **3b**, for which we give the optimized structure in Figure 2B. During the rotation the remaining degrees of freedom were optimized. The structure **3b** represents an energy minimum with a positive Hessian matrix. In the rotation the role of the $\Pi_{SiH_3}{}^x$ and $2\sigma_{SiH_3}$ orbitals are interchanged. That is, the $\Pi_{SiH_3}{}^x$ orbital is now responsible for the Ti–Si σ-interactions in 1a′ (**6a**) and 2a′ (**6b**), whereas $2\sigma_{SiH_3}$ is responsible for the back-donation

$1a' = 2a_1 + \Pi^x_{SiH_3} + 1s_H$ $\qquad$ $2a' = 1b_1 + \Pi^x_{SiH_3}$

6a $\qquad$ 6b

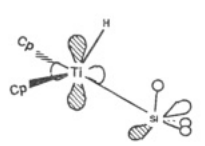

$3a' = 1a_1 + 2\sigma_{SiH_3}$

6c

to the metal center in 3a′ (**6c**). However, bonding in the two conformers **3a** and **3b** is quite similar except for this interchange. The 1a′, 2a′, and 3a′ orbitals of **3a** and **3b**, respectively, are correlated in Figure 1.

It follows from Figure 3A, where we display the reaction profile for the process in eq 5, that the rotation **3a** → **3b**

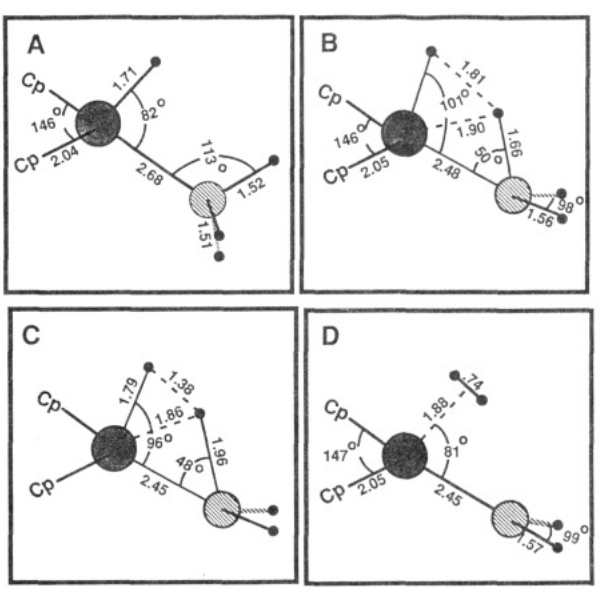

Figure 2. Optimized structures for (A) $Cp_2Ti(H)(SiH_3)$ of conformation **3a**, (B) $Cp_2Ti(H)(SiH_3)$ of conformation **3b**, (C) the approximate transition state for the migration process **3b** → **3d**, and (D) the optimized silylene dihydrogen adduct **3d**.

has an enthalpy of 32 kJ mol^{-1} and an activation barrier of 53 kJ mol^{-1}. The profile for the step **3a** → **3b** was, as already specified, obtained by a linear transit procedure, and the calculated value for the barrier represents, as a consequence, an upper bound for the actual barrier. It follows from the optimized structure of **3b** given in Figure 2B that the H_a atom now is close enough (R(Ti–H_a) = 1.90 Å) to the Ti center for an agostic interaction. The agostic

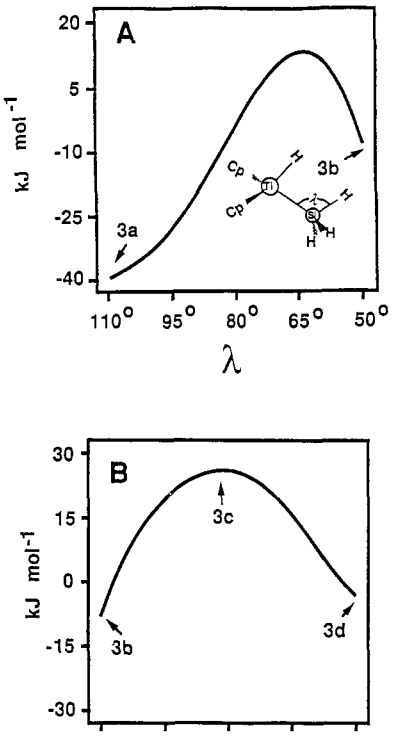

Figure 3. Reaction profile for (A) the rotation step **3a** → **3b** and (B) the migration step step **3b** → **3d**.

interaction is particularly pronounced in **6a**. Note further that the Si–H_a bond distance has been elongated to 1.66 Å.

The remaining part of the process in eq 5 was modeled by a migration, **3b** → **3c** → **3d**, of the H_a atom toward the H_d ligand with the formation of silylene dihydrogen adduct, **3d**. During the migration all remaining degrees of freedom were optimized. The correlation of the 1a′, 2a′, and 3a′ orbitals during the migration process, **3b** → **3c** → **3d**, is given in Figure 1. It follows that the 1a′ orbital correlates with the (largely) H_2 σ-orbital (**7a**) of the silylene

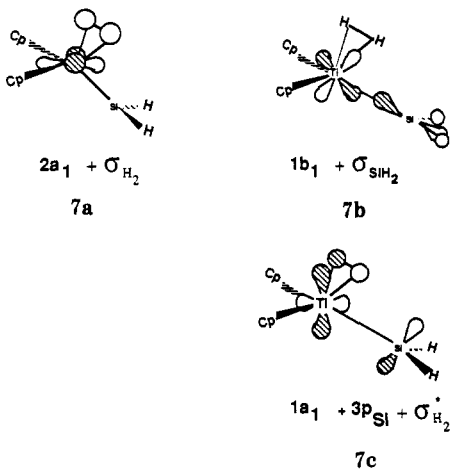

dihydrogen intermediate **3d**, whereas 2a′ (**7b**) becomes the Ti–silylene σ-bonding orbital (**5a**) and 3a′ (**7c**) the Ti–silylene π-bonding orbital (**5b**). The 3a′ (**7c**) orbital is further stabilized in **3d** by the interaction with the σ*-orbital of H_2. The profile for the migration, obtained by a linear transit as specified above, is given in Figure 3B, and the structures of the approximate transition state **3c** as well as the silylene dihydrogen adduct **3d** are given in Figure 2. It should be pointed out that the transition-state structure **3c** is approximate since it is found from a linear transit rather than from a search for an energy extremum

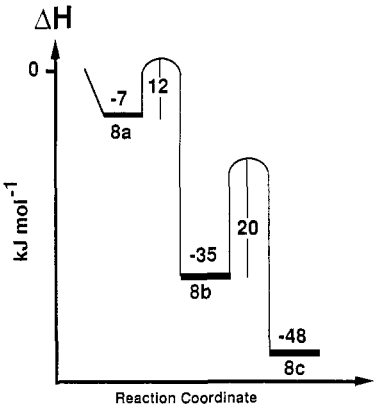

Figure 4. Schematic reaction profile for the reaction **8a** → **8c**.

with one negative force constant. The migration step is seen to have a modest reaction enthalpy of 8 kJ mol^{-1} with an activation barrier of only 33 kJ mol^{-1}. Part of the reason for the low activation barrier is the fact that the 1s orbital on the migrating H_a atom can have a stabilizing interaction with the empty $1a_1$ (**2a**) and $2a_1$ (**2c**) orbitals of Cp_2Ti in the transition state **3c**, where R(Ti–H_a) = 1.86 Å (see Figure 1).

The adduct **3d** between H_2 and $Cp_2Ti(SiH_2)$ represents the last stage in the reaction of eq 5 before H_2 is eliminated. The adduct **3d**, in which the H–H distance has reached the value of free H_2, is only held together by 3 kJ mol^{-1}. We note further that the $Cp_2Ti(SiH_2)$ framework in **3d** (see Figure 2D) largely has reached the geometry of the free silylene complex $Cp_2Ti(SiH_2)$ (**3e**).

V. Addition of SiH_4 to Cp_2TiSiH_2

The addition process in eq 6 represents the reverse of eq 5 in that a σ-bond now is added rather than eliminated. The process in eq 6 has been modeled in a way similar to that for eq 5.

We allow first for the formation of the σ-adduct **8a** between SiH_4 and the silylene complex **3e**. The adduct **8a** has a modest calculated formation energy of only 7 kJ mol^{-1} as is indicated in Figure 4, where we give the energy profile for the reaction in eq 6.

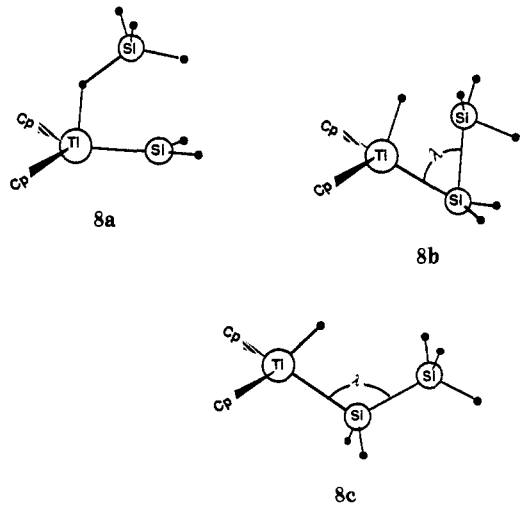

We allow in the next stage of the process the silyl group to slide toward the silylene with the formation of the intermediate **8b**. The optimized structure for **8b**, which represents an energy minimum with a positive Hessian matrix, is given in Figure 5A. The silyl group in **8b** is seen to have close bonding distances to the central metal, R(Ti–Si) = 2.63 Å, and the hydride, R(Si–H) = 1.78 Å, as

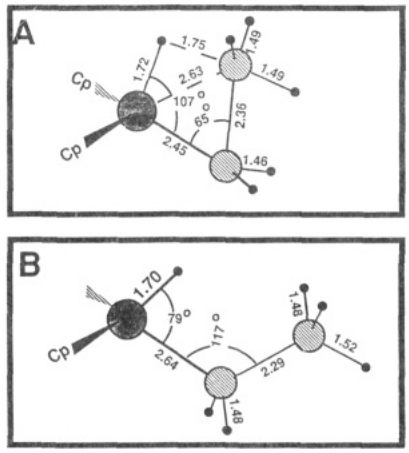

Figure 5. Optimized structures for (A) $Cp_2Ti(H)(SiH_2SiH_3)$ of conformation **8b** and (B) $Cp_2Ti(H)(SiH_2SiH_3)$ of conformation **8b**.

well as to the silylene, R(Si–Si) = 2.35 Å. The two Ti–Si σ-bonds are established in the orbitals **9a** and **9b** from

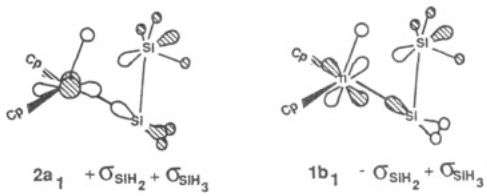

9a **9b**

bonding interactions between $2\sigma_{SiH_3}$ and σ_{SiH_2} and respectively $2a_1$ and $1b_1$ of the Cp_2Ti fragment. Note that the SiH_3 group is rotated in such a way as to allow for the two σ-interactions in **8a** and **8b**. The Si–Si σ-bond is established between $3p_{Si}$ of the SiH_2 group and $\Pi_{SiH_3}{}^{x}$ of SiH_3 in **9d**, whereas the Ti–H bond stems from the interaction in **9c** between $1s_H$ and $1a_1$.

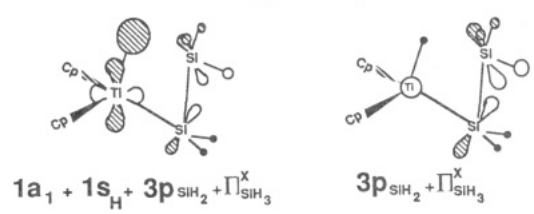

9c **9d**

We calculate the passage **8a** → **8b** to be exothermic with ΔH = −28 kJ mol^{-1}. The corresponding barrier was determined, from a linear transit, to be 12 kJ mol^{-1} (see Figure 4).

The last step, **8b** → **8c**, in the process of eq 6 represents an opening of the λ angle from λ = 65° in **8b** to λ = 117° in **8c**, with the formation of the hydrido silyl complex **8c**. The optimized structure for **8c** is given in Figure 5B. The passage **8b** → **8c** was calculated to be exothermic by 13 kJ mol^{-1} with a barrier of 20 kJ mol^{-1} (see Figure 4).

VI. Concluding Remarks

We have here evaluated one of the possible mechanisms for the polymerization of primary organosilanes by a titanocene-based catalyst. The polymerization process is, as already mentioned, nearly thermoneutral with the enthalpy in eq 2 given by ΔH_2 = 14 kJ mol^{-1}. It is thus reasonable to assume that the reaction is driven by the removal of H_2.

The key step in the mechanism proposed by Harrod for the polymerization of primary organosilanes by a titanocene-based catalyst is the chain propagating process in eq 9. The estimated enthalpy for the reaction in eq 9 is

$$Cp_2Ti(H)(SiH_2R) + SiH_3R \rightarrow Cp_2Ti(H)(SiHRSiH_2R) + H_2 \quad (9)$$

identical with that of the polymerization process in eq 2 with $\Delta H_{2a} = 2[D(\text{Si–H})] - D(\text{H–H}) - D(\text{S–Si}) = 14$ kJ mol^{-1}. Our calculated enthalpy for the model reaction

$$Cp_2Ti(H)(SiH_3) + SiH_4 \rightarrow Cp_2Ti(H)(SiH_2SiH_3) + H_2 \quad (10)$$

was −8 kJ mol^{-1}.

We have visualized the chain propagating reaction in eq 9, modeled here by the process in eq 10, as taking place in two steps. The first step (eq 5) is an α-hydride elimination from the SiH_3 group with subsequent loss of H_2 to give the $Cp_2Ti{=}SiH_2$ silylene. This step was calculated to have a reaction enthalpy of 40 kJ mol^{-1}. The second step is an addition (eq 6) of SiH_4 to Cp_2TiSiH_2, for which we calculate an enthalpy of −48 kJ mol^{-1}.

It is clear from our findings that the feasability of the proposed mechanism (eqs 5 and 6) depends on whether or not one can expect the endothermic step in eq 5, with a calculated enthalpy of 40 kJ mol^{-1}, to take place at ambient temperatures. We feel that this might very well be the case for two reasons. In the first place, the step in eq 5 can be driven by the removal of H_2, just as in the overall polymerization process of eq 2, which also is endothermic. In the second place, the step in eq 5 is dissociative. This could well lead to a $T\Delta S$ contribution to ΔG_{3a} of −40 kJ mol^{-1} with the result that $\Delta G_{3a} \approx 0$.

A number of other possible mechanisms for the polymerization reaction exist. It should, however, be noted that all such mechanisms would have endothermic steps since the overall polymerization process is endothermic. Among the more likely alternative mechanisms for the formation of the Si–Si bonds in this type of reaction are σ-bond metathesis (eq 11)[26] and the insertion of a disilene, formed by β-hydride elimination from a metal silyl complex (eq 12).[27,28]

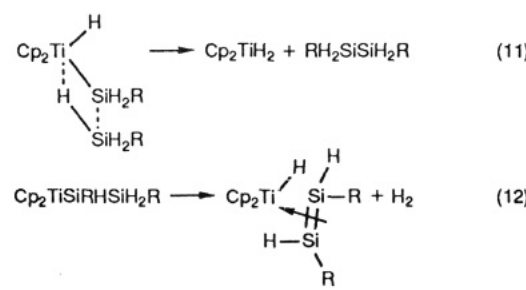

Acknowledgment. This investigation was supported by the Natural Sciences and Engineering Research Council of Canada. We thank the University of Calgary for access to their Cyber-205 computer installations.

(26) σ-bond metathesis has been suggested as a possible mechanism: Tilley, T. D. Personal communication. The endothermicity in such a mechanism would, at least in part, come from the endothermic hydrogen loss from the metallocene dihydride.

(27) Although mononuclear disilene complexes are thus far unknown, a dimeric platinum complex with a bridging group that appears to be a disilene species was recently reported.[28]

(28) Zarate, E. A.; Tessier-Youngs, C.; Youngs, W. *J. Am. Chem. Soc.* **1988**, *110*, 4068.